Desalination 431 (2018) 86–99

Contents lists available at ScienceDirect

Desalination

journal homepage: www.elsevier.com/locate/desal

Fouling indicators for field monitoring the effectiveness of operational strategies of ultrafiltration as pretreatment for seawater desalination

Han Gu[a], Anditya Rahardianto[a,b], Larry X. Gao[a], Xavier Pascual Caro[c], Jaume Giralt[c], Robert Rallo[d], Panagiotis D. Christofides[a,*], Yoram Cohen[a,b,**]

[a] Water Technology Research Center, Department of Chemical and Biomolecular Engineering, University of California, Los Angeles, CA 90095-1592, United States
[b] Institute of the Environment and Sustainability, University of California, Los Angeles, CA 90095-1592, United States
[c] Departament d'Enginyeria Química, Universitat Rovira i Virgili, Av. Països Catalans 26, 43007 Tarragona, Catalunya, Spain
[d] Departament d'Enginyeria Informàtica i Matemàtiques, Universitat Rovira i Virgili, Av. Països Catalans 26, 43007 Tarragona, Catalunya, Spain

GRAPHICAL ABSTRACT

Real-Time Monitoring of UF Fouling Indicators.

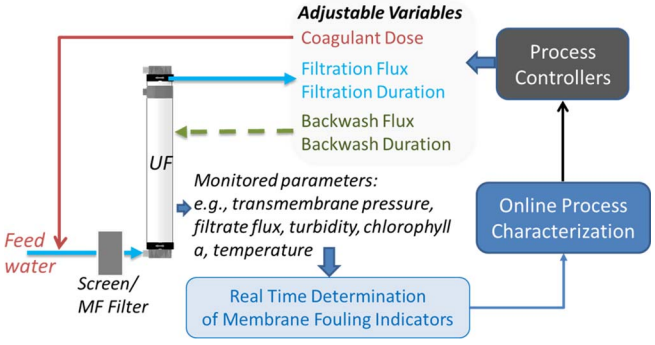

ARTICLE INFO

Keywords:
Ultrafiltration
Backwash
Fouling indicators
Reverse osmosis
Seawater desalination

ABSTRACT

The applicability of fouling indicators for real time performance assessment of UF feed pretreatment in RO seawater desalination was explored in a field study using an integrated seawater UF-RO desalination pilot plant. Fouling indictors were evaluated with respect to quantification of UF backwashability, unbackwashed fouling resistance and UF fouling rate. Feed water quality and coagulant dose demonstrated measurable impact on both UF fouling rate and effectiveness of foulant removal via UF backwash. Increased coagulant dose promoted higher rate of cake formation and in turn improved backwash efficiency. However, there was a maximum coagulant dose beyond which there was no further backwash improvement. Backwash effectiveness increased with higher backwash flux and duration, up to threshold upper limits, but declined as the filtration period increased above a threshold limit. Field tests during periods of temporally varying feed quality demonstrated that higher fouling rate (promoted by inline coagulation) resulted in more effective backwash and correspondingly lower progressive rise in post-backwash UF resistance. The study results suggest that real-time UF fouling indicators, based on UF filtration resistance metrics and backwash effectiveness, should be potentially useful for tracking UF performance and thus for deployment of UF feed-back control for optimal performance of UF feed pretreatment.

* Corresponding author.
** Correspondence to: Y. Cohen, Water Technology Research Center, Department of Chemical and Biomolecular Engineering, University of California, Los Angeles, CA 90095-1592, United States.
E-mail addresses: pdc@seas.ucla.edu (P.D. Christofides), yoram@ucla.edu (Y. Cohen).

https://doi.org/10.1016/j.desal.2017.11.038
Received 11 September 2017; Received in revised form 24 November 2017; Accepted 25 November 2017
Available online 08 December 2017
0011-9164/

1. Introduction

Dwindling fresh water supplies from traditional sources, such as ground and surface water, coupled with frequent drought conditions across the globe, intensify the need to develop alternative and sustainable potable water supplies [1–3]. In recent years, seawater and brackish water desalination and water reuse technologies have been implemented in various regions of the U.S. and around the globe as part of the movement to diversify the portfolio of available water resources. In the generation of the above non-traditional water resources reverse osmosis (as well as nanofiltration) membrane technology is often utilized for desalination and as a barrier against multiple contaminants. However, membrane fouling is a major challenge for effective operation of both seawater and brackish water RO plants [4–7]. In the absence of effective RO feed water pretreatment, membrane fouling by particulate/colloidal matter, biofoulants, extracellular polymeric substances (EPS) that are abound in seawater (particularly in littoral water) [8–10] and organics degrades membrane performance (e.g., reduced permeability and thus increased applied pressure requirement for a given target flux, decreased permeate quality), increase the frequency of required chemical cleaning and consequently shortening of membrane longevity and as a consequence increased water treatment cost [11–14]. Therefore, RO feed water pre-treatment is critical for (complete or partial) removal of potential foulants such as particulates, colloids, and organic matter [5,6,9,11].

In recent years, ultrafiltration (UF) has emerged as an effective method for pre-treatment of RO feed water compared to conventional feed pre-treatment options (e.g. sand filters, cartridge filters) [6,9,15–18]. UF membranes having a pore size typically in the range of 0.1–0.01 μm can remove particulates, colloids, microorganisms and some dissolved organics matter (often with the aid of coagulant dosing), and accordingly producing high quality filtrate. Both UF filtration and backwash effectiveness [19] can often be improved through coagulant dosing of the UF feed [10,12,20]. Coagulant dosing promotes floc formation (i.e., aggregation of fine particles and colloidal matter), thereby improving both UF and MF membrane filtration and hydraulic cleaning [21–24]. Given the above attributes, UF is becoming increasingly the choice method for RO feed water pre-treatment, particularly since UF membrane permeability loss (due to fouling) can be recovered with periodic backwashing and/or air scouring [15,25,26].

UF foulants that are not removed during backwash result in UF irreversible fouling. When the buildup of irreversible fouling reaches a critical level (e.g., as indicated by increased transmembrane pressure for constant flux operation) and backwash is no longer effective in providing sufficient membrane permeability restoration chemical cleaning-in-place (CIP) is utilized [27,28]. However, plant operational costs (e.g., due to chemical costs and possible productivity loss) can increase significantly with increased CIP frequency [29,30]. Therefore, it is critical to optimize both UF filtration and backwash [31–33]; thus, efforts have been devoted to elucidate the impact of various factors on UF fouling and backwash effectiveness such as, for example, feed water quality [19,22], filtration period length [34], backwash flux [32,35], duration and frequency, backwash water composition [36,37], coagulant dosing, CIP strategies, and membrane properties [19,28,38,39].

A number of studies have proposed the use of fouling indices such as the Silt Density Index (SDI) and various forms of Modified Fouling Index (MFI) to quantify the feed water “fouling potential” [28,40–52] via measurements of flux decline through a surrogate membrane ex-situ. These fouling indices rely on off-line measurements and thus an inherent lag time relative to real-time UF system behavior. A large number of the studies on fouling indices studies with UF as well as MF systems did not consider coagulant dosing and have relied on synthetic saline, surface water or seawater blended with organic foulants [28,41,43–45,49,50,52–55]. Evaluation of seawater and algal-rich surface water UF fouling potential, associated with green and blue algae, was also recently investigated via real time fluorometeric measurements of chlorophyll-*a* [12,56–59]. These studies with laboratory-scale hollow fiber UF membrane setup demonstrated significant correlation of chlorophyll-*a* with UF membrane flux decline due to biofilm growth.

Invariably, arriving at effective UF filtration and backwash strategies requires tracking of the extent of UF fouling and assessment of backwash effectiveness. Conventional UF operations rely on tracking of UF fouling via the UF transmembrane pressure (TMP), UF filtration resistance or membrane permeability normalized with respect to their initial value in the filtration step just post CIP [10,22,26,60–63]. Such approaches, however, do not lend themselves to cycle-to-cycle tracking of backwash efficiency nor quantifying the contributions of reversible (i.e., backwashable) and irreversible (i.e., unbackwashable) fouling to UF resistance in progressive filtration cycles.

UF fouling is a complex phenomenon that is governed by water quality and temperature which can be temporally variable, as well as operating conditions. Therefore, in order to establish optimal UF operating conditions with effective process control [64,65], there is a need to develop real-time fouling indicators. Previously, backwash triggering controller, based on a maximum allowable filtration resistance change per cycle ($\Delta R_{T,max}$) was proposed and demonstrated as an effective and practical method to control backwash frequency [34]. Subsequent work demonstrated that real-time quantification of backwash efficiency, along with determination of the associated of coagulant dosing, can be utilized for determination of optimal coagulant dose adjustment in response to changing UF fouling as affected by varying feed water fouling potential [19]. However, assessing UF performance, with respect to the progression of fouling and backwash effectiveness, is complex as it requires real time quantification of multiple fouling indicators based on plant sensors' data.

The present work aimed to elucidate the complex relationship between various UF operational variables and UF fouling behavior as observed under field conditions for UF treatment of RO seawater feed water. Accordingly, a framework for online UF fouling metrics (or indicators) were determined to assess cycle-to-cycle filtration and backwash fouling and permeability recovery (or fouling resistance removal), respectively. The UF filtration period and fouling rate (FR), unbackwashed and post-backwash UF resistances (ΔR_{UB} and R_{PB}, respectively), and UF backwash efficiency (BW_{eff}) were determined in real-time for each filtration/backwash cycle over both short and long-term field tests. The above fouling metrics were then assessed with respect to filtration and backwash flux and duration coagulant dose and in relation to feed water turbidity and chlorophyll-*a* measurements in both the UF filtrate and feed water. The correlations between the UF system operational variables and the above fouling indicators can form the basis for performance forecasting and development of UF self-adaptive control.

2. Experimental

2.1. Integrated UF-RO system

The UF-RO seawater desalination system (Fig. 1) consisted of directly integrated UF and RO skids (i.e., without an intermediate UF or RO feed tank). The designed maximum system feed water capacity was 190.8 m^3/day (50,400 GPD) operating at a maximum RO unit recovery of 35% recovery (equivalent to desalted water production of 66.8 m^3/day (17,640 GPD)). Details of the integrated UF-RO system are available elsewhere [34]. Briefly, the UF skid comprised of an inline basket strainer (0.32 cm ID perforation, Hayward SB Simplex, Clemmons, NC), a 200 μm self-cleaning microfilter (TAF-500, Amiad Corp., Mooresville, NC), and three inside-out polyethersulfone (PES) multi-bore hollow fiber membranes (0.02 μm pore size) UF modules (Dizzer 5000 +, Inge, Greifenberg, Germany) arranged in parallel with each nodule having membrane surface area of 50 m^2.

Feed water to the UF modules was delivered by a feed pump (XT100

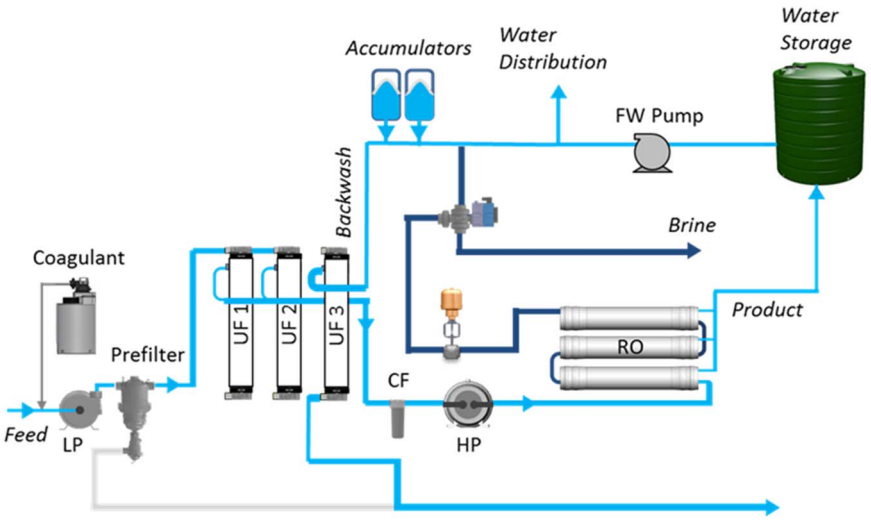

Fig. 1. Schematic diagram of the UF-RO pilot system. (LP: low pressure feed pump, HP: high pressure positive displacement pump, CF: carbon filters for added RO protection).

SS, 3.73 kW, Price Pump, Sonoma, CA) controlled by a variable-frequency drive (VFD) (VLT AQUA Drive FC202, Danfoss, Denmark). Inline coagulants dosing was achieved by direct injection into the UF feed stream (prior to the UF feed pump) via a metering pump (Grundfos, DDA 7.5-16, Bjerringbro, Denmark). UF module filtrate flow rates were monitored using magnetic flow meters (Signet 2551, George Fischer Signet, Inc. El Monte, CA) and pressure was monitored via sensors (AST4000, American Sensor Technologies, Mt. Olive, NJ) installed on the feed and filtrate sides of the UF modules. A turbidity meter (Signet 4150, Georg Fischer Signet LLC, El Monte, CA), fluorometer sensor (Turner Designs, Cyclops-7 2108, San Jose, CA), pH meter (Sensorex S8000CD, EM802/pH, Garden Grove, CA), and a temperature sensor (Signet 2350-3, George Fischer Signet LLC, El Monte, CA) were installed on the UF filtrate line. Banks of electrically actuated 2 and 3 way ball valves (Type 107, 2-ways, Georg Fischer LLC, Irvine, CA and TEBVA6-1 3-way, Plast-O-Matic Valves, Inc. Cedar Grove, NJ) enabled switching between filtration and backwash mode, and changing filtration/backwash directions (top or bottom) for the individual UF modules [66].

The UF filtrate was delivered to the RO high pressure positive displacement feed pump (APP 10.2, Danfoss, Nordborg, Denmark) with a high efficiency motor (CEM4103T, 25 hp., TEFC, Baldor, Fort Smith, AR) and Variable Frequency Drive (VFD) control (VLT AQUA Drive FC 202, 22 kW, Danfoss, Nordborg, Denmark). The RO feed pump, with an outlet flow and pressure ranges of 66–170 L/min and 2–8 MPa, respectively, provided feed to three seawater (99.65% salt rejection) spiral-wound RO elements membranes (Dow Filmtec SW30HRLE-400, the Dow Chemical Company, Midland, MI) each housed in one of three separate pressure vessels arranged in series.

In the specialized arrangement of the integrated UF-RO system, RO concentrate was available for direct backwash of the UF modules, through a continuous stream as well as via high flux pulse backwash using two 3 L bladder type hydraulic accumulators (C111ND, Blacoh Fluid Control, Riverside, CA, USA) [32]. In addition, RO permeate was collected in a 1136 L water storage tank with provision for diverting the permeate water for UF freshwater backwash using a centrifugal pump (CME5-4A, Grundfos, Denmark). Upon triggering of UF backwash, the UF membranes are taken offline sequentially and individually backwashed. It is noted that at all times at least two modules remain in filtration mode. In the above operational mode, a filtration and backwash sequence, which includes all three UF modules, is considered a complete UF filtration cycle.

2.2. Field study

The field study was conducted at the Naval Facilities Engineering and Expeditionary Warfare Center (NAVFAC-EXWC) at Port Hueneme, CA. Raw surface seawater was pumped directly from the port to a 7571 L (2000 gal) holding tank (< 3 h detention time), and used as feed to the UF-RO system. The range of intake water quality during the study is shown in Table 1. In the above area algal blooms and red tide events are common during spring and summer seasons [67,68]. It is noted that the feed water to the UF unit was not chlorinated and that UF backwash was without chemical additives.

Effective UF control strategies require suitable fouling indicators that quantify UF performance and backwash effectiveness based on real-time monitoring of process parameters (target filtrate flux which in turns affects transmembrane pressure, feed water turbidity, chlorophyll-*a* and temperature). Moreover, such fouling indices should provide a clear correlation with critical UF operational variables such as filtration and backwash duration and flux and coagulant dose (Fig. 2). Accordingly, the present study proceeded along three sequential phases aimed at quantifying fouling indicators (Section 3.1). The first phase of the study focused on the effect of inline coagulation on the progression of UF fouling, filtration fouling rate and UF backwash performance. Two coagulants were tested over a range of doses of 1.5–4.9 mg/L as Fe^{3+} and 2.8–25 mg/L as Al^{3+} for $FeCl_3$ and ACH, respectively, for fixed filtration duration for tests that consisted of least 64 filtration/backwash cycles. In the second phase, short term experiments were conducted, a fixed coagulant dose, to evaluate the impact of backwash flux, backwash duration and backwash frequency on UF performance. These tests were carried out over operational period of 15–60 min, typically consisting of 12 filtration/backwash cycles. At the end of each of these short duration tests, the UF modules were backwashed at a high flux (162 L/m^2 h, approximately 3.6 times the filtration flux) for two

Table 1
Range of seawater feed quality at field study location (2012–2015).

Feed water property parameters	Range
Chlorophyll-*a*	12–400 (μg/L)
pH	7.5–8.2
Total dissolved solids (TDS)	33,440–36,800 mg/L
Total organic carbon (TOC)	0.7–1.3 mg/L
Temperature	11.2–25.6 °C
Turbidity	1.1–19 NTU

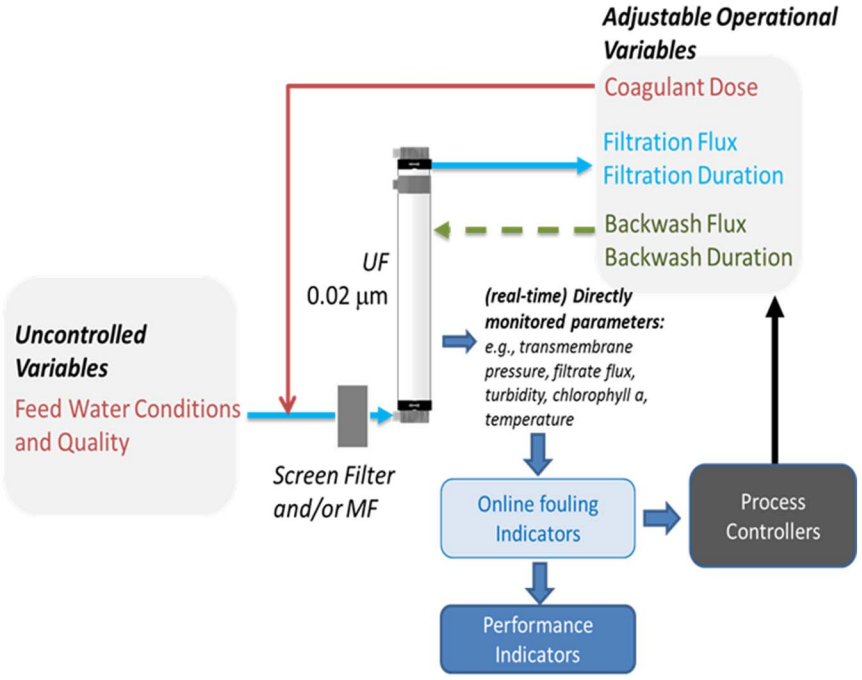

Fig. 2. Schematic depiction of UF process variables that are uncontrolled and those that are adjustable for optimizing UF operation.

minutes, using RO permeate.

The third phase focused on longer term (> 240 h) field tests in which the various fouling indicators were quantified to characterize UF filtration and backwash performance under field conditions in which temporal variability of raw feed water was observed.

3. Online UF fouling characterization

3.1. Online fouling and performance indicators selection

UF pretreatment of RO feed water is generally carried out under constant filtration flux operation in a "dead-end" mode. The UF filtrate flux J_F (m/s) is typically expressed as [69]:

$$J_F = \frac{\Delta P}{\mu R_t} \tag{1}$$

where μ is the feed water viscosity (Pa·s), ΔP is the transmembrane pressure drop (*kPa*), and R_t is the total membrane hydraulic resistance that is typically expressed by the resistance-in-series model [70],

$$R_t = R_m + R_{cake} + R_{irr} \tag{2}$$

in which R_m, R_{cake}, and R_{irr} are the clean membrane hydraulic, cake and irreversible resistances, respectively. Here R_{cake} refers to the foulant layer that can be removed by hydraulic backwash; this removable foulant portion is regarded as the cake layer that builds on the membrane surface. For constant flux operation, the UF membrane resistance increases with progressive fouling over the course of a filtration cycle (Fig. 3). When the UF membrane resistance reaches a prescribed threshold level, backwash is triggered to remove the foulant layer and thus recover the membrane permeability (Fig. 3). The UF foulant layer portion not removed (unbackwashed) in the backwash step may remain as "irreversible" fouling or may be removed to some degree in subsequent backwash cycles. Backwash effectiveness can thus be quantified by the degree of removal of the foulant layer as quantified by the reduction (or removal) of membrane resistance.

For a given filtration cycle *n*, the initial UF resistance ($R_{initial,n}$) (i.e., post-backwash resistance for cycle n-1), filtration duration (Δt_n) and final UF filtration resistance ($R_{final,n}$) are determined from the UF filtration resistance data. The UF fouling resistance increase for a given cycle n, $\Delta R_{T,n}$ (i.e., $R_{final,n}$ - $R_{initial,n-1}$) can be expressed as the sum of the resistance removed by the previous backwash period ($\Delta R_{BW,n} = R_{final,n} - R_{initial,n}$) and the unbackwashed resistance (i.e., not removed) by UF backwash ($\Delta R_{UB,n} = R_{initial,n} - R_{initial,n-1}$) (Fig. 3):

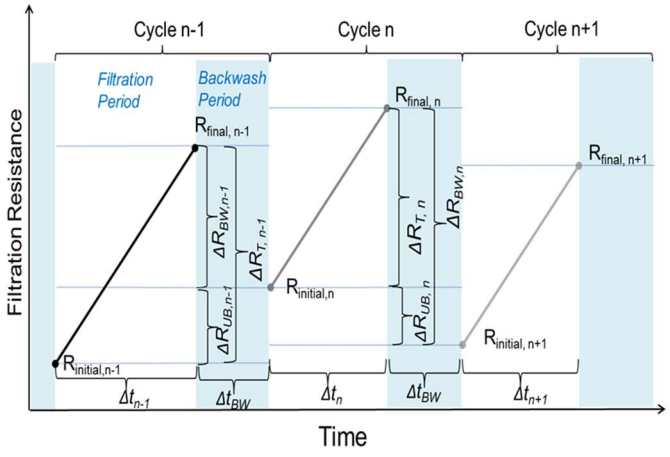

Fig. 3. Illustration of filtration/backwash cycles. $R_{initial,n}$ and $R_{final,n}$ are the initial and final UF membrane resistances, respectively ($\Delta R_{T,n} = R_{final,n} - R_{initial,n}$) for cycle *n* filtration duration of Δt_n, and $\Delta R_{UB,n}$ is the cycle *n* unbackwashed portion of the membrane fouling resistance buildup from cycle *n-1*. ($R_{initial,n}$ also represents the post-backwash resistance associated with cycle *n-1* and $\Delta R_{BW,n} = \Delta R_{T,n} + \Delta R_{UB,n}$).

$$\Delta R_{T,n} = \Delta R_{UB,n} + \Delta R_{BW,n} \tag{3}$$

The change in $\Delta R_{UB,n}$ with progressive filtration/backwash cycles is indicative of the effectiveness of foulant cake removal by backwash. In principle ΔR_{UB} can be negative (i.e., $\Delta R_{UB} \gg R_{irr}$) which would be the case when the degree of foulant removal, in a given cycle, is higher relative to the previous cycle (e.g., due to improved water quality and environmental factors). In characterizing UF filtration performance, the fouling rate for the given filtration cycle *n* (FR_n) is a fouling indicator for the filtration step,

$$FR_n = \frac{\Delta R_{T,n}}{\Delta t_n} \tag{4}$$

Recent work has demonstrated that rapid fouling, during the

filtration step can be promoted by inline UF feed coagulant dosing. Coagulation promotes the formation of particle aggregates (or flocs) larger in size than the original smaller suspended solids which favors the formation of a foulant cake layer, while reducing the potential for membrane pore plugging. It is important to recognize that when conventional coagulation/sedimentation treatment is employed prior to UF filtration, FR_n may be higher or lower than UF treatment without coagulation. Moreover, unlike conventional coagulation/sedimentation, as shown in recent work, inline coagulation is effective in promoting a foulant cake layer that is more easily backwashed [19,23], and providing a protective layer to reduce the likelihood of pore plugging. Moreover, the fouling rate, as quantified by FR_n, is expected to be higher for UF filtration with inline coagulant dosing relative to UF operation without coagulation [19,71].

The progression of UF fouling (as measured by post-backwash (*PB*) UF resistance for each cycle, i.e., $R_{PB,n} = R_{initial,n+1}$), over many filtration/backwash cycles, and the ability to reduce the rate of *PB* resistance increase relies on the ability to minimize the cycle-to-cycle unbackwashed membrane resistance ($\Delta R_{UB,n}$). Backwash efficiency ($BW_{eff,n}$), which here is defined as the percentage of removed resistance for a given cycle,

$$BW_{eff,n}(\%) = \frac{\Delta R_{BW,n}}{\Delta R_{T,n}} = 1 - \frac{\Delta R_{UB,n}}{FR_n \cdot \Delta t_n} \tag{5}$$

depends on both $\Delta R_{T,n}$ and $\Delta R_{UB,n}$. With progressive filtration/backwash cycles, the rise in post-backwash initial filtration resistance (R_{PB}) is given by:

$$R_{PB} = \sum_{n=0}^{N} (R_{PB,n-1} - R_{initial,n-1}) = \sum_{n=0}^{N} \Delta R_{UB,n} = R_{initial,N} - R_{initial,0} \tag{6}$$

where R_{PB}, which is indicative of the overall state of the UF membrane fouling, is the summation of the cycle-to-cycle UF unbackwashed resistance change, and where $R_{initial,N}$ and $R_{initial,0}$ are the final post-backwash and initial UF membrane filtration resistances, respectively. The need for membrane CIP can be established based on a maximum allowable threshold R_{PB} for the UF module (e.g., as per the manufacturer recommendation of the maximum recommended transmembrane pressure for a given filtration flux).

When UF backwash is accomplished using the RO concentrate, the fraction of recovered UF filtrate (Y_{UF}) is complete (i.e., $Y_{UF} = 1$). However, when a portion of the UF filtrate is stored and utilized for backwash, UF recovery for a given cycle n ($Y_{UF,n}$) is reduced to a level governed by the backwash flux and frequency as given by:

$$Y_{UF,n} = 1 - \left(\frac{J_{BW} \cdot \Delta t_{BW}}{2 \cdot J_F \cdot \Delta t_n} \right) \tag{7}$$

in which Δt_{BW} is the backwash time (h) and J_{BW} is the backwash flux (L/m^2 h), and where the total filtrate recovery at the end of *N* cycles ($Y_{UF,N}$) is given as:

$$Y_{UF,N} = 1 - \left(\frac{N \cdot J_{BW} \cdot \Delta t_{BW}}{2 \cdot \sum_{n=1}^{N} J_F \cdot \Delta t_n} \right) \tag{8}$$

Higher Y_{UF} can be achieved by maximizing filtrate production (e.g. higher filtration flux, reduced backwash frequency and system offline period) while minimizing backwash flux, duration and frequency. It is noted that in typical UF systems where UF filtrate is used for backwash UF recovery is reported to be in the range of 85–95%.

The utility of the different fouling metrics (FR_n, $\Delta R_{T,n}$, $\Delta R_{UB,n}$, BW_{eff} and R_{PB}) for control decisions regarding UF operation would clearly rely on establishing their correlation with UF operational performance and backwash efficiency as conceptualized in Fig. 4. The overall control objectives are to reduce the rate of *PB* resistance rise in order to lengthen the time (t_{cc}) before the need for CIP is reached (i.e., when the maximum allowed transmembrane pressure drop for the UF module of ~100 kPa is reached), while also increasing the achievable UF filtrate recovery (Y_{UF}). An informed UF operational decision would then require real-time determination of the degree by which the adjustable process variables can reduce the adverse change in the target fouling indicators.

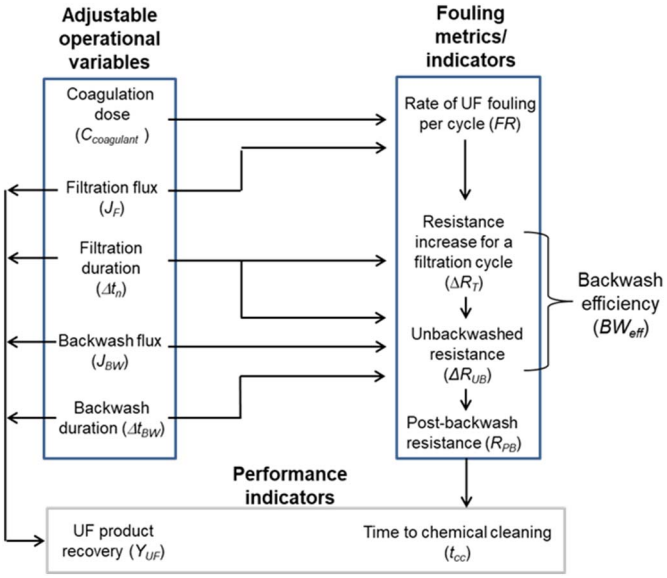

Fig. 4. Causal relationship diagram of the links between UF adjustable operational variables and fouling indicators. Arrows from operational variables point toward a fouling or performance indicator indicate a direct cause-effect relationship.

3.2. Group averaged data analysis

Sensor data from field operation is affected by feed water quality and environmental conditions (e.g., feed water temperature), in addition to noise arising from natural fluctuation of sensor signals, actuators and pump operation. Therefore, a moving average was adapted for data processing over a minimum of 6 filtration/backwash cycles to quantify the average filtration period fouling rate $\langle FR \rangle_j$, unbackwashed resistance $\langle \Delta R_{UB} \rangle_j$, average resistance increase per filtration period $< \Delta R_{T,n} >$, and backwash efficiency $\langle BW_{eff} \rangle_j$, while the overall progression of the post-backwash UF resistance $< R_{PB} >$ was assessed based on averaging of at least 6 cycles. A summary of the fouling indicators and their physical process implications is provided in Table 2.

4. Results & discussion

4.1. Filtration resistance monitoring

In the operation of the UF system, membrane backwash was triggered by an online control system once the incremental UF resistance increase in a given filtration period, ΔR_T, exceeded a threshold value, as per the approach described previously [34]. The feed seawater filtration period for seawater pretreatment was typically of the order of 20–50 min, and the membrane filtration resistance (Fig. 5) increased linearly (i.e., constant rate of fouling) over this period. As illustrated in Fig. 5, the UF post-backwash resistance (i.e., the initial UF filtration period resistance) progressively increased with continual operation; however, the UF post-backwash resistance for a given cycle was also observed to decrease at times, relative to the previous cycle. Such a behavior should not be surprising since membrane rate of fouling and backwash effectiveness are governed by multiple factors including, for example, coagulation, filtration and backwash conditions, feed water chemistry quality and environmental conditions (e.g., temperature). The fact that post-backwash UF resistance can both increase or decrease

Table 2
Summary of fouling indicators[a].

Online fouling indicators	Description	Cycle-to-cycle fouling metric calculation (n^{th} cycle, over N cycles)	Averaged fouling metric for jth segment (over N cycles)	Notes
Filtration period fouling rate (FR)	Rate of filtration resistance buildup (per cycle)	$FR_n = \frac{R_{T,n}}{\Delta t_n}$	$\langle FR \rangle_j$	Directly related to feed fouling potential
Backwash efficiency (BW_{eff})	Portion of filtration resistance removed	$BW_{eff,n} = \frac{\Delta R_{BW,n}}{\Delta R_{T,n}} = 1 - \frac{\Delta R_{UB,n}}{FR_n \cdot \Delta t_n}$	$\langle BW_{eff} \rangle_j$	Relative measurement of backwash efficiency
Unbackwashed resistance	Resistance not removed by backwash	$\Delta R_{UB,\,n} = \Delta R_{T,\,n} - \Delta R_{BW,\,n}$	$\langle \Delta R_{UB} \rangle_j$	Absolute measurement of initial resistance change per cycle
Post-backwash resistance	Current state of UF fouling	$R_{PB} = \sum_{n=0}^{N} (R_{ini,n} - R_{ini,n-1}) = \sum_{n=0}^{N} R_{PB,n}$	$\langle R_{PB} \rangle_j = \sum_{j=1}^{J} \langle R_{PB} \rangle_j$	Equivalent to change in initial resistance

[a] Fouling indictors were determined in real-time based on monitored process variables (Section 3.1).

over the course of a system operation is critical to ascertain in real time. Such information can be utilized to implement proper feedback controls strategies not only with respect to backwash adjustment strategies (e.g., backwash duration and flux), but also with respect to real time coagulant dose optimization [19].

4.2. Effect of coagulants dose on filtration period fouling rate and UF backwash effectiveness

Inline coagulation increases floc size, thereby improving the effectiveness of particulate matter removal. At the same time, inline coagulation also leads to higher rate of membrane fouling via cake formation, while at the same promoting increased backwash efficiency [19]. Therefore, in order to provide information needed for real-time coagulant dose optimization it is necessary to establish the relationship between fouling indicators and coagulant dose. Indeed, based on a series of tests shown in Fig. 6, the average UF fouling rate in a filtration cycle (FR_n) clearly increases with increased coagulant dose. In this example it is also evident that the coagulant $FeCl_3$ resulted in a higher fouling rate (by about a factor of 3.5) relative to ACH. A higher fouling rate and higher coagulant dose would lead to a greater foulant cake layer thickness, following the same linear rise as the fouling rate, as shown in the inset of Fig. 6; the cake layer thickness was estimated based on a cake formation model for constant flux operation [69] (Appendix A, Supplementary Material). With increased inline coagulant dose membrane fouling is expected to shift toward the formation of a cake layer, which is not adhered to the surface, and can be backwashed more effectively than foulants that adsorb onto the membrane and/or plug its pores. Here it is noted that jar testing clearly showed that flocs

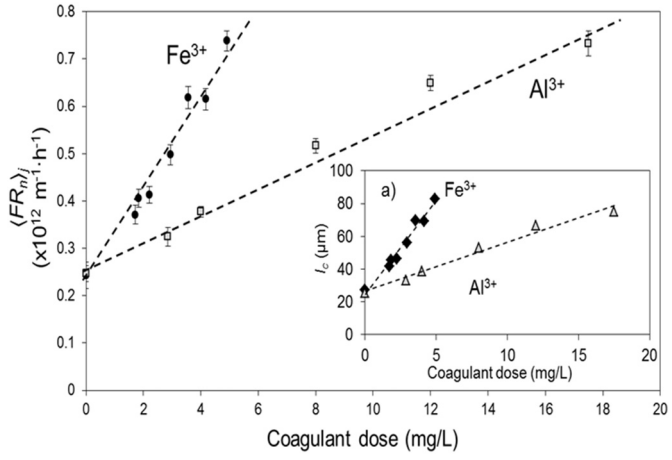

Fig. 6. Dependence of UF membrane fouling rate (quantified as the rate of change in membrane filtration resistance, FR) during filtration on inline coagulant dose (using Fe^{3+} or Al^{3+}). UF operating conditions: Filtration flux of 45.4 L/m^2·h for 30 min followed by 70 s backwash at a flux of 162 L/m^2 h. The vertical error bars indicate standard deviation for the fouling rate averaged over 64 cycles. The inset figure shows the change in the UF fouling layer cake thickness (l_c) with coagulant dose for both Fe^{3+} and Al^{3+}.

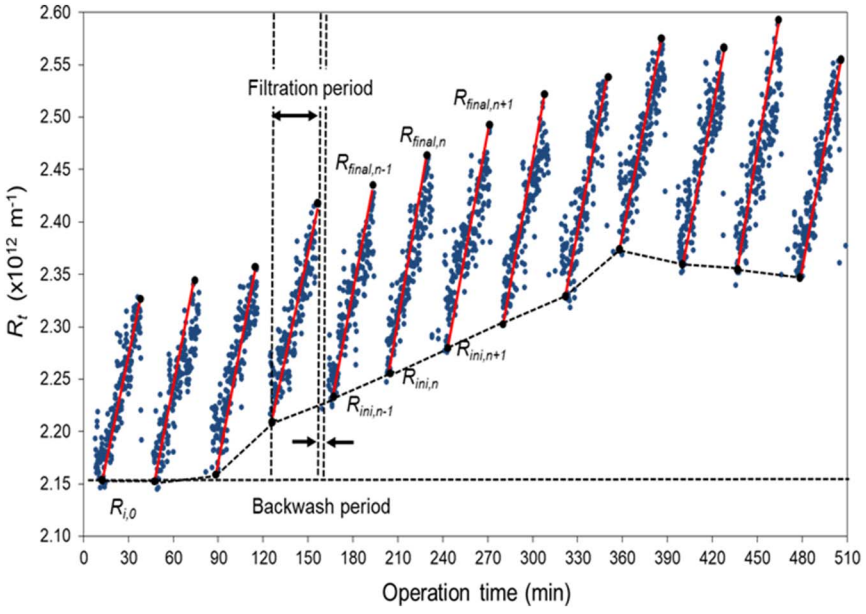

Fig. 5. Illustration of UF operation displaying membrane resistance during multiple filtration/backwash cycles. The solid lines represent the fitted linear regression lines. $R_{i,o}$ is the initial UF resistance at the start of the run (*0th* cycle), $R_{ini,n}$ and $R_{final,n}$ are the UF membrane resistances at the beginning and end of filtration cycle n. The dashed line traces the post-backwash resistance. UF operating conditions: Filtration flux 45.4 L/m^2·h for a duration of 29–30.4 min with inline $FeCl_3$ coagulant dosing of 2.20 mg/L Fe^{3+}, followed by 70 s backwash at a flux of 162 L/m^2 h. Feed turbidity and chlorophyll-a levels were in the range of 0.46–0.73 NTU and 67.2–155 μg/L, respectively.

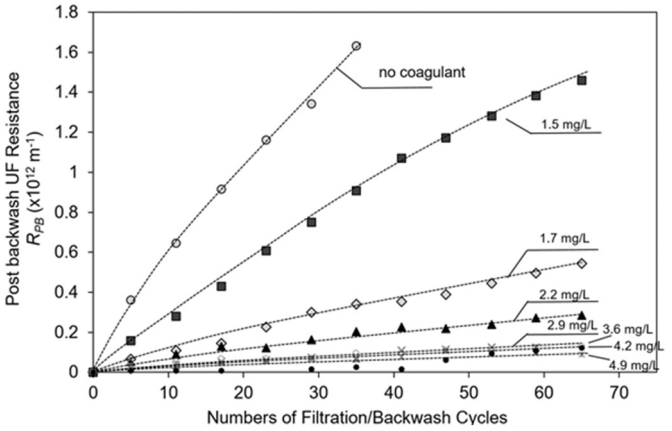

Fig. 7. Assessment of post-backwash UF resistance for various Fe^{3+} coagulant doses. UF operating conditions: Filtration flux of 45.4 L/m^2 h with backwash triggering every 30 min (for a period of 70 s) at a flux of 162 L/m^2 h. Feed turbidity during the 1.3 day experimental period was in the range of 0.45–1.32 NTU with chlorophyll-*a* being in the range of 32–78 μg/L.

formed using ACH were visually smaller and finer than the flocs formed by $FeCl_3$.

The impact of inline coagulant feed dosing on backwash effectiveness was assessed by quantifying the post-backwash resistance, R_{PB} (averaged over a set of six filtration/backwash cycles) over a series of short-term tests over an operational period of ~1.3 days during which water quality did not change appreciably (Fig. 7). As expected, R_{PB} progressively increases with increasing cumulative number of filtration/backwash cycles. However, R_{PB} decreased significantly when coagulant dosing was introduced, implying greater backwash effectiveness at higher dose. For example, after 36 cycles, with 1.5 mg/L Fe^{3+} coagulant dosing, R_{PB} decreased by factor of 1.8 and further decreased, by a factor of 64 with coagulant dose of 4.9 mg/L. It is clear from Fig. 7, however, and consistent with previous work [19], that the benefit of inline coagulation reaches a level above which further coagulant decreases has little or no advantage for reducing R_{PB}. For example, after 36 cycles, as the coagulant was increased from 3.6 to 4.9 mg/L, R_{PB} decreased by about 20%. A similar R_{PB} behavior was observed for the case of ACH dosing as detailed in the Supplementary Material (Fig. C1, Appendix C).

Over the course of UF operation it should be expected that R_{PB} will eventually increase up to a threshold that will require chemical cleaning in place (CIP) (Section 3.1). Accordingly, the operational period up to CIP requirement (Fig. 8) can be projected based on the slope of R_{PB} with respect to time (Fig. 7) past about 40 filtration/backwash cycles where CIP would be required when the UF membrane filtration resistance reaches ~9.63×10^{12} m^{-1} (estimated based on the maximum allowed UF transmembrane pressure, Section 3.1). Such an estimate, however, is only an approximation as it is premised on operation that is at the same conditions as for the above tests and with the same water quality as in the above tests. For example, as shown in Fig. 8, for the lowest overall fouling rate of 0.587×10^9 m^{-1} h^{-1} at coagulant dose of 4.17 mg/L Fe^{3+} CIP would be required every 77 days. In contrast, with the ACH coagulant, even at a dose range of 12–25 mg/L, CIP would be required every 1–4 days. The above field tests suggest that $FeCl_3$ is a more effective coagulant in promoting higher fouling rate during filtration and correspondingly higher backwash effectiveness (i.e., lower remaining residual or unbackwashed UF resistance).

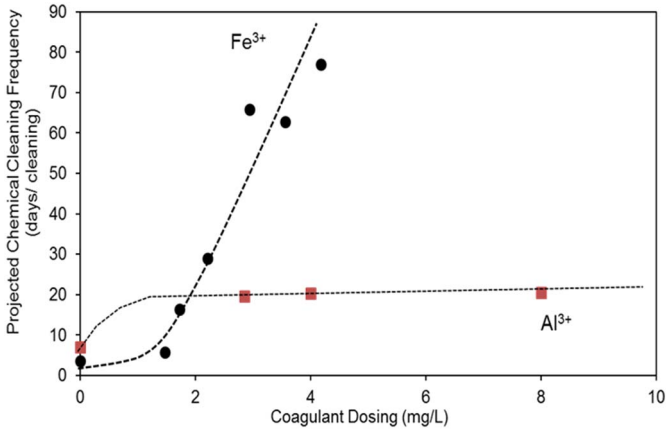

Fig. 8. Projected chemical frequency (days per chemical cleaning) for two different coagulants ($FeCl_3$ and ACH). UF operating conditions: Filtration flux of 45.4 L/m^2 h with backwash triggered every 30 min, at a flux of 162 L/m^2 h for 70s duration. Initial (clean) UF membrane resistance: 4.76×10^{11} m^{-1}. Threshold (maximum allowable) UF membrane resistance that triggers needed chemical cleaning: 9.63×10^{12} m^{-1}.

4.3. Effect of coagulants dose on UF backwash efficiency (BW_{eff})

A direct quantification of UF backwash efficiency, BW_{eff} (Eq. 5), can be illustrated by inspecting the behavior in ΔR_{UB} relative to total resistance increase per cycle (ΔR_T). As shown in Fig. 9, the unbackwashed resistance decreases with increased coagulant dose which can also be viewed by the increased backwash efficiency (Eq. 5, averaged here over 64 cycles). It is postulated that at a higher rate of fouling (Section 4.2), which is facilitated increasing the coagulant dose, cake formation will be with larger flocs that are more easily removed via backwash. Indeed, as seen in Fig. 9, as the coagulant dose increases backwash efficiency correspondingly increases. For example, inline coagulation with $FeCl_3$ at 4.16 mg/L as Fe^{3+} would increase backwash efficiency to 99.7% relative to 95% at coagulant dose of 1.7 mg/L as Fe^{3+} and to 90% without coagulant dosing. Inline coagulation with ACH required higher dose to attain similar levels of backwash efficiencies. For example, to attain backwash efficiency of 97.9% ACH coagulant dose of 2.85 mg/L as Al^{3+} would be required, but a significantly higher dose of 12 mg/L would be needed to attain 99% efficiency.

As observed in Fig. 9, there is an apparent threshold beyond which further coagulant dose increase did not lead to measurable backwash efficiency increase. This threshold was about 4.16 mg/L Fe^{3+} and 12 mg/L Al^{3+} for inline coagulation with $FeCl_3$ and ACH, respectively. Here it is important to state that overdosing should be avoided to avert coagulant passage to the RO elements. It is stressed that under conditions of temporally variable water feed quality the optimal coagulant dose will change. Therefore, both for achieving optimal UF operation and for reducing coagulant use one would have to utilize a suitable coagulant dose controller, as demonstrated recently in [19].

Ultrafiltration along with inline coagulation promotes the formation of larger aggregates (or flocs). As a consequence, membrane cake formation (Section 4.2) is more rapid which then renders backwash more effective. Accordingly, one should expect that with increased filtration cycle fouling rate (promoted by adjustment of the coagulant dose), the unbackwashed resistance (ΔR_{UB}) would decrease, thereby reducing the buildup of irreversible fouling. It is interesting to note that the trend is similar for both coagulants (Fig. B3, Appendix B, Supplementary Material) suggesting similar degree of cake formation for a given filtration fouling rate. It is apparent that above a filtration period fouling rate threshold ($FR \sim 0.4 \times 10^{-12}$ (m h)$^{-1}$ for the present case) the unbackwashed fouling resistance was no longer reduced with progressive filtration/backwash cycles. This behavior is expected given that there is a threshold coagulant dose (Fig. 9) above which the unbackwashed resistance (ΔR_{UB}) reaches its lowest value (i.e., maximum backwash efficiency) and given that the fouling rate varies linearly with coagulant dose (Figs. 6).

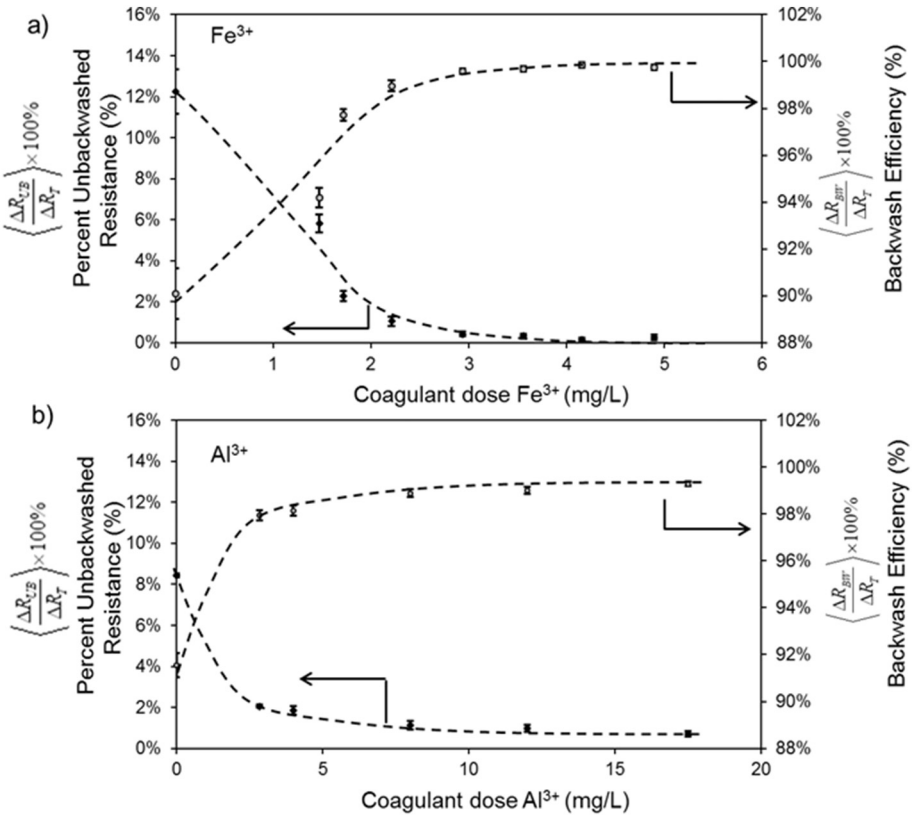

Fig. 9. Impact of UF inline coagulation dose, for the coagulants $FeCl_3$ and ACH, on UF backwash efficiency (BW_{eff}). UF system was operated at filtration flux of 45.4 L/m^2 h for 30 min, followed by backwash at a flux of 162 L/m^2 h for 70 s.

4.4. Effect of backwash conditions on UF backwash effectiveness (BW_{eff})

Backwash effectiveness is impacted by UF filtration and backwash conditions in addition to coagulant dose (Section 4.3). An illustration of the dependence of backwash effectiveness (average over 12 cycles) on filtration period length, backwash flux and duration is provided in Fig. 10, for UF operation at fixed $FeCl_3$ coagulant dose of 4.17 mg/L as Fe^{3+}. For a given filtration flux (36.9 L/m^2 h) and backwash flux and duration (70 s), backwash efficiency was essentially 100% until a threshold filtration period of 40 min was reached beyond which backwash effectiveness declined to nearly 82%. Backwash effectiveness decreased somewhat (by ~29%) as the filtration flux increased from ~33 to 42 L/m^2 h. It is postulated that, over the above feasible range of filtration flux needed to maintain effective RO operation for the present plant, increased filtration flux was accompanying by a shorter convective residence time for effective inline coagulation and thus lower fouling rate and hence lower backwash effectiveness (Fig. B3, Appendix B, Supplementary Material).

For a given filtration conditions, increasing the backwash flux increases backwash effectiveness up to a plateau after which there is little or no benefit in further increase in backwash flux (Fig. 10b). For example, upon increasing the backwash flux from 70 L/m^2 h (about a factor of 1.9 greater than the filtration flux of 36.9 L/m^2·h) by about 200% (or a factor of 3.8 higher than the filtration flux) BW_{eff} increased from 50% to 99.9%. For a given UF filtration flux and duration, the UF backwash efficiency can also be increased, for a given backwash flux, by lengthening the backwash duration (Fig. 10c). For example, for the current UF-RO system, upon increasing the backwash duration, from 12 min to 80 min, the backwash efficiency increased from about 78% to about 95%. It is noted that an upper limit was reached with respect to backwash duration beyond which there was no further improvement of backwash effectiveness.

4.5. Real-time monitoring of UF fouling indicators in seawater feed pretreatment

A series of three UF operational field tests of 5–12 days in duration were undertaken in order to evaluate the fouling indicators under conditions during which water quality may vary to different extents (Fig. 11). In these field tests UF backwash was triggered based on the self-adaptive approach [34] described in Section 3.1. Field Test #1 was conducted over a period of 12 days of continuous UF-RO operation. Feed turbidity was in the range of 0.65–4.9 NTU with chlorophyll-*a* in the UF feed and filtrate being in the range of 42–101 μg/L and 0.48–0.54 μg/L, respectively (Fig. 11a–c). During the above period the average filtration duration was about 21 min with a total of 812 filtration/backwash cycles. For the above test period, the unbackwashed ($\langle \Delta R_{UB} \rangle$) and post-backwash resistance ($\langle R_{PB} \rangle$), and backwash efficiency ($\langle BW_{eff} \rangle$), and fouling rate (*FR*), all averaged over 24 cycles, are shown in Figs. 12a–d. During the first day of operation there was an initial period during which the residual unbackwashed resistance (Fig. 12a) increased during the first day and then after about 2 days of operation at $0.030 \pm 0.025 \times 10^{12}\ m^{-1}$. The above trend is likely to have occurred due to foulant cake compaction and distribution of coagulant throughout the three UF modules (Fig. 1). The post-backwash UF resistance (Fig. 12b) increased with time due to progressive buildup of fouling resistance owing to the accumulation of residual unbackwashed UF resistance (Fig. 12a). It is noted that the fouling rate (Fig. 12c) during the filtration periods was relatively constant ($0.48 \pm 0.07 \times 10^{12}\ m^{-1}\ h^{-1}$) suggesting that the temporal fluctuations in feed quality did not lead to significant alteration of the severity of cycle-to-cycle membrane fouling rate, with the exception of the first day of rapid fouling. Given the above, it is not surprising that the UF backwash efficiency, which was initially ~60%, increased during the first two day of operation and thereafter remained relatively stable at

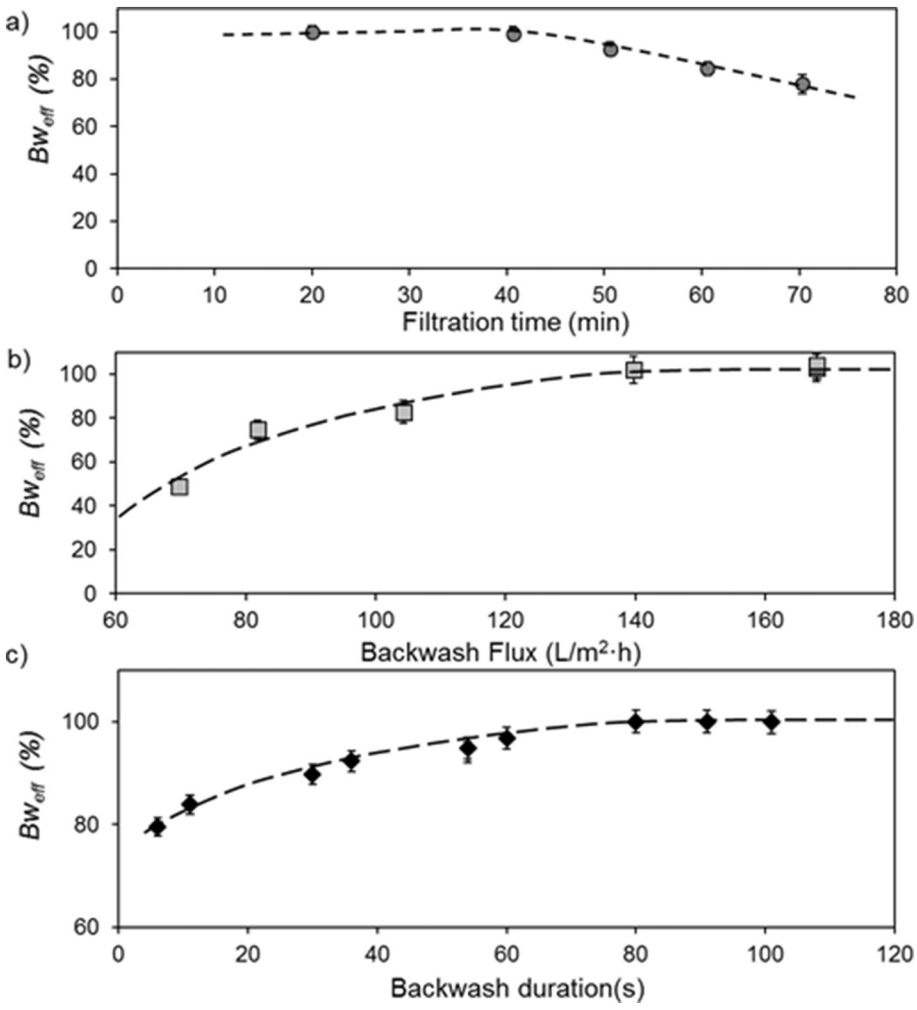

Fig. 10. Dependence of backwash effectiveness on: a) filtration duration for operation at filtration flux of 36.9 L/m^2 h and backwash flux of 162 L/m^2 h of 70 s; b) backwash flux for UF operation at filtration flux of 36.9 L/m^2 h for 30 min, followed by backwash for a period of 70 s; c) backwash duration for UF operation at filtration flux and period of 36.9 L/m^2 h and 30 min, respectively, and backwash flux of 162 L/m^2 h. Note: All tests were conducted with inline $FeCl_3$ coagulant dosing of 4.17 mg/L as Fe^{3+}.

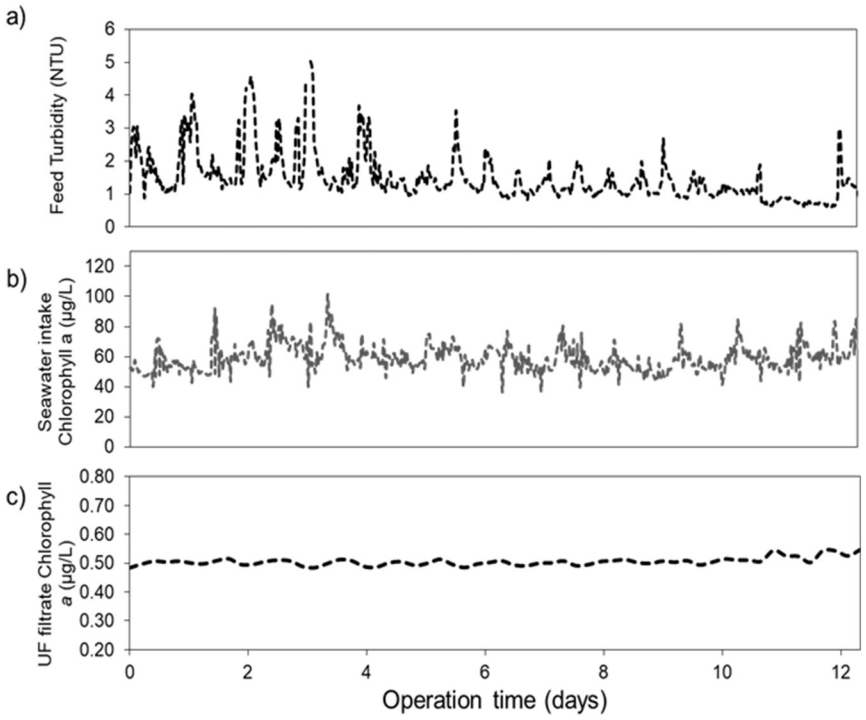

Fig. 11. Water quality data during Test #1 over a period of 12 days (300 h). Feed turbidity: 1.46 ± 0.05 NTU. Chlorophyll-*a*, feed: 59.7 ± 0.73 µg/L, filtrate: 0.50 ± 0.04 µg/L.

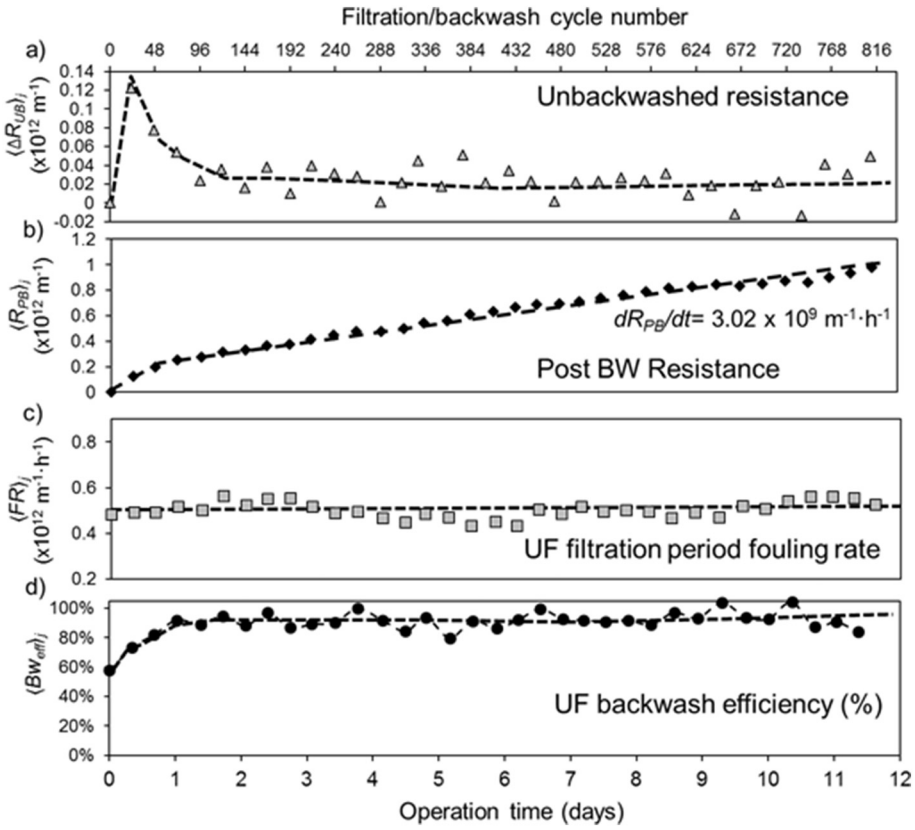

Fig. 12. Variation of UF fouling indicators over a 12 day period during which water quality varied as per Fig. 11 (Test #1). UF operation was in self-adaptive mode of backwash triggering, whereby filtration duration was in the range of 29–42 min at a flux of 45.4 L/m^2 h with inline $FeCl_3$ coagulant dosing of 4.12 mg/L Fe^{3+}, backwash flux was 162 L/m^2 h for a period of 70 s.

$\langle BW_{eff} \rangle$ = 95.2% ± 1.0% (Fig. 12d). Finally, it is noted that for the above operation, the post-backwash fouling rate (i.e., dR_{PB}/dt) for the UF system (Fig. 12b) was ~3.02 × 10^9 m^{-1} h^{-1} which implies that the system can be operated for 126 days before the need for CIP.

A follow-up field Test #2 was conducted over a period of about 5 days (UF operation of 482 filtration/backwash cycles). During the above period feed water turbidity was in the range of 1.25–3.24 NTU (Fig. 13a), and the UF feed and filtrate chlorophyll-*a* concentrations (Fig. 13b,c) were in the range of 20–127 μg/L and 0.41–0.66 μg/L, respectively. In this test the UF filtration and backwash fluxes were the

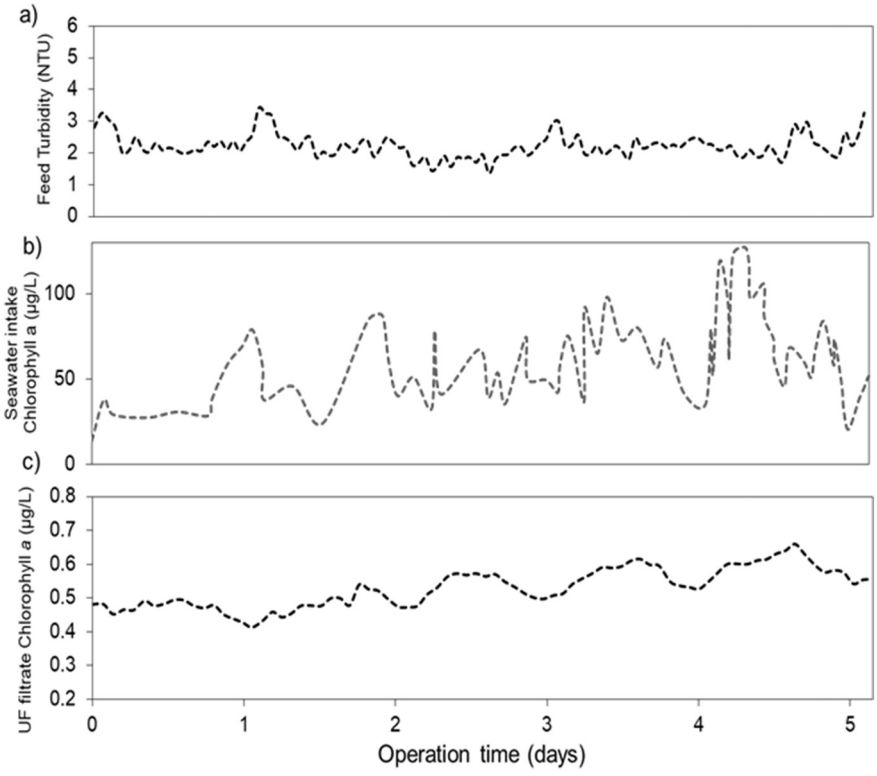

Fig. 13. Feed water turbidity and chlorophyll *a* in the UF feed and filtrate for 25 h (~5 days) of field Test #2. Feed turbidity: 2.22 ± 0.07 NTU, feed and UF filtrate *chlorophyll-a*: 60.4 ± 5.8 μg/L and 0.53 ± 0.01 μg/L, respectively.

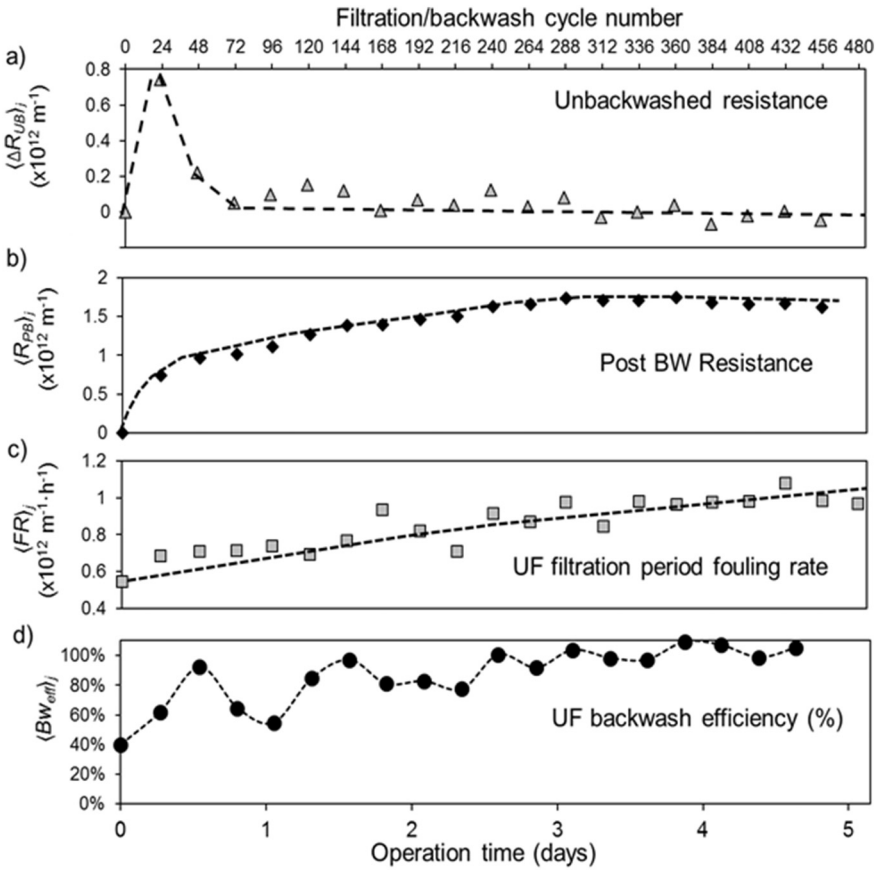

Fig. 14. Variation of UF fouling indicators over the 125 h (~5 days) of Test #2 during which water quality varied as given in Fig. 13. UF operation was in self-adaptive mode of backwash triggering (total of 479 filtration/backwash cycles), whereby filtration duration was in the range of 25–33 min at a flux of 45 L/m^2 h with inline coagulant dosing of $FeCl_3$ of 4.2 mg/L Fe^{3+}, backwash flux was 162 L/m^2 h for a period of 70 s.

same as in Test #1 with backwash also triggered in a self-adaptive mode (Section 3.1). In Test #2, as in Test #1, the unbackwashed UF resistance increased rapidly from the initial level of no residual resistance to a maximum value of $0.74 \times 10^{12}\ m^{-1}$ after an operational period of 6.5 h (Fig. 14a), but then decreased to a value of $\sim 0.079 \times 10^{12}$ by day 3 with an apparent slight temporally decreasing slope (i.e., $d\langle \Delta R_{UB} \rangle / dt \approx -0.59 \times 10^{9} m^{-1} h^{-1}$). Although the post-backwash resistance increased as expected during the initial 3 days (Fig. 5b), there was a slight decrease (~7.5%) from day 3 to day 5. This behavior should not be surprising since the filtration cycle fouling rate (Fig. 14c) increased monotonically from the initial value of $\sim 0.55 \times 10^{-12}\ m^{-1} h^{-1}$ by a factor of 1.8 over the test period over the five day period. Given that the feed turbidity was relatively stable (1.25–3.24 NTU) (Fig. 13a), it is unlikely that particulate matter was responsible for the progressive increase in the filtration period fouling rate. This observation is consistent with the findings of other studies that turbidity measurements alone are insufficient for assessing the feed water fouling potential. We note, however, that the feed chlorophyll-*a* varied considerably (20–127 μg/L; Fig. 13b) and appeared to be elevated over the operational period of 40 to 120 h. The detection of chlorophyll-*a* implies the presence of algae which was likely the cause of higher filtration period fouling rate (Fig. 14c). However, for system operation under adaptive backwash control [34], at higher filtration period fouling rate backwash was triggered at a higher frequency (Supplementary Materials, Figs. F1–F2). As a result, the UF filtration period decreased from 32.5 min to 25 min by the end of the test period. It is also noted that backwash efficiency is expected to increase with rising per cycle fouling rate, for operation under inline coagulant dosing (Section 4.3); this was indeed the case in this field Test showing that the backwash efficiency increased over the course of the field test from the initial value of 40% to about 99% (Fig. 14d).

Test #3 was conducted during a period in which there was a storm event that commenced in day 2 of the UF operation (about 53.5 h after the test started). The feed water turbidity and chlorophyll-a data which were previously reported in [19] are reproduced in Fig. 15a. At day 4 of the 6.5 day test period both turbidity and chlorophyll-*a* spiked to values of about 15.3 NTU and 152 μg/L, respectively, which were significantly higher, by factors of 14.4 and 1.64, relative to the initial values at the beginning of the test period. Thus, Test #3 presented a unique opportunity to evaluate the fouling indicators with respect to the observed UF performance under poor feed water quality conditions. Test #3, which was conducted under adaptive backwash triggering, was part of an earlier demonstration of UF operation with a coagulant dose controller as described in [19]. In this test the coagulant controller was activated (Fig. 15b-e) 62.4 h after the beginning of the storm event (i.e., $t = 62.4$ h). Prior to the storm event the feed water turbidity was < 1.0 NTU and chlorophyll-*a* was in the range of 80–100 μg/L (and ~0.64 μg/L in the UF filtrate, Appendix F and Fig. G1, Supplementary Material), and where the filtration period fouling rate, $\langle FR \rangle$, was in the range of 0.45–0.7 $\times 10^{12}\ m^{-1}$. UF post-backwash resistance increased steadily, due to the progressive accumulation of unbackwashed UF resistance, rising to about 8% above the initial state during the storm. However, due to the increase in inline coagulant dose, the filtration period fouling rate increased enabling the backwash effectiveness to increase from the post-storm value of 80% ± 7% to exceeding 100% during the storm. The latter behavior indicates that UF resistance removal was not only complete relative to the previous set of cycles, but that foulant not removed in previous cycles was also removed. The filtration period fouling rate stabilized after day 5 (at $\sim 1.51\ m^{-1} h^{-1}$) and the post-backwash UF resistance actually decreased which is consistent with both a high UF backwash efficiency and the improvement in feed quality. Throughout the field tests UF filtrate turbidity was maintained at 0.03 ± 0.005 NTU (Fig. G1, Appendix G, Supplementary Material) and the RO unit, operating at a recovery level of 36%,

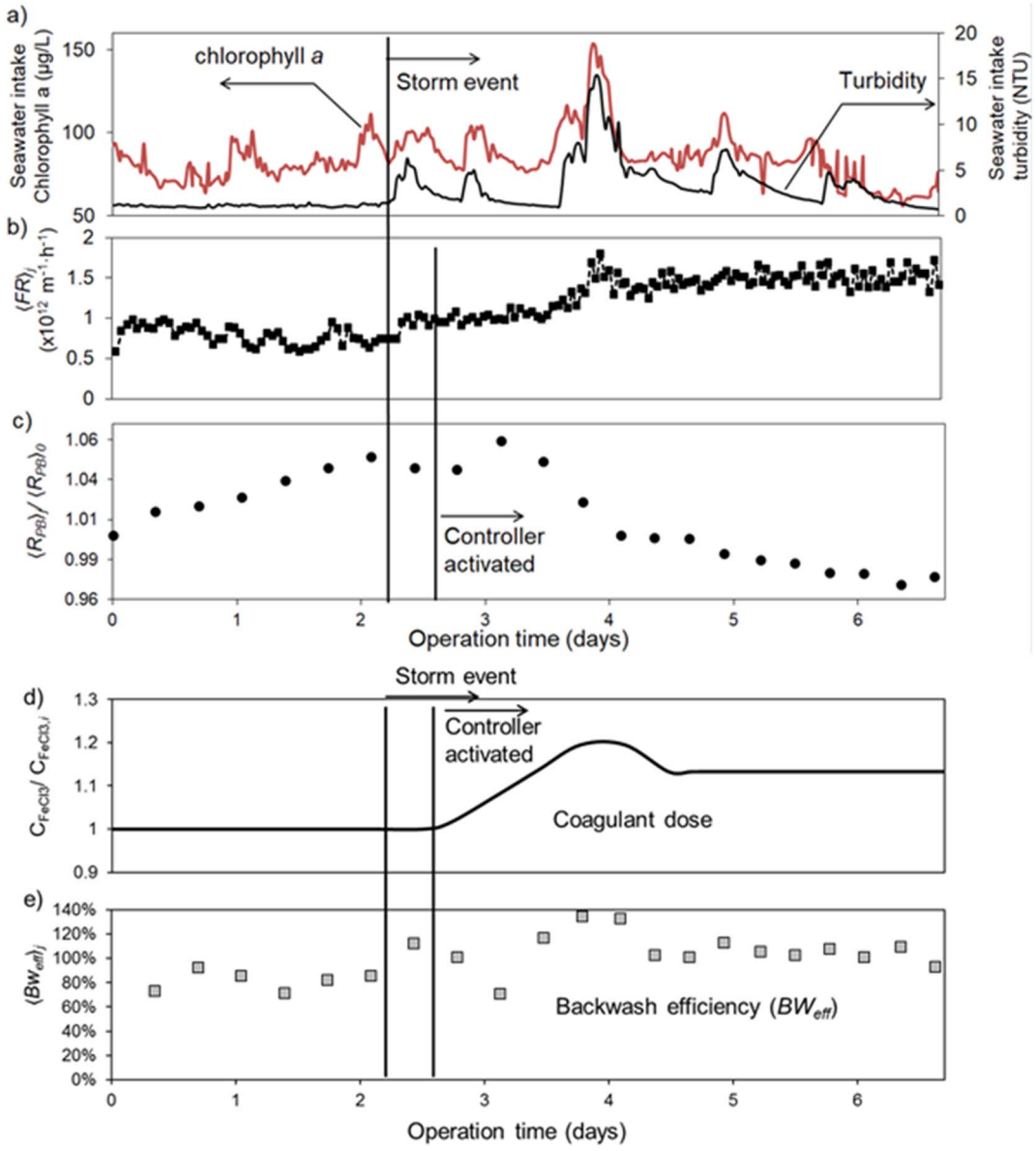

Fig. 15. UF system fouling indicators during Test #3 in which a storm event was experienced. UF operating conditions: Filtration flux of 45 L/m^2 h with $FeCl_3$ inline coagulant dosing of 4.2 mg/L Fe^{3+}, with adaptive backwash (resulting in filtration periods of 25–45 min) at a flux of 162 L/m^2 h for a period of 70 s.

produced permeate of salinity of 148 ± 13 mg/L total dissolved solids. It is also noted that the RO membrane elements did not reveal any signs of fouling and their permeability remained stable at 1.85 ± 0.137 × 10^{-12} m/Pa s.

5. Conclusions

Real-time monitoring of UF fouling behavior in the treatment of raw seawater feed for RO desalination was explored using fouling indicators that included filtration period fouling rate, unbackwashed and post-backwash resistances, as well as backwash efficiency. Field evaluation of the above parameters was carried out for seawater UF pretreatment of RO feed water. In a series of systematic short-term tests inline coagulation was shown to increase the rate of fouling; this in turn reduced the unbackwashed resistance and increased backwash efficiency. $FeCl_3$ was a more effective coagulant relative to ACH in promoting higher backwash efficiency and thus projected to allow longer UF operation before requiring chemical cleaning. The range of coagulant dose for achieving effective filtration and backwash was in the range of ~2.9–4.9 mg/L Fe^{3+} with backwash efficiency increasing with coagulant dose; above coagulant dose of 4.9 mg/L Fe^{3+} there was essentially no improvement of backwash efficiency. The maximum backwash period was about 70s beyond which backwash improvement was marginal, and the effective backwash flux at the above backwash period was about 140 L/m^2 h.

For a given UF operation, at a given filtration flux and inline coagulant dose, backwash effectiveness increased with backwash flux and duration up to a threshold upper limit, but decreased for filtration periods above a threshold limit. Field tests over periods of days, during which water quality was variable (with respect to monitored turbidity and chlorophyll-*a*), conclusively showed that increased fouling rate indeed resulted in higher backwash efficiency and thus a lower progressive increase of UF post-backwash resistance. The results of the current study suggest that the real-time UF fouling indicators (based on direct UF performance metrics) can provide useful insight regarding UF operation and thus be utilized to guide and implement self-adaptive operational control for effective UF pretreatment.

Nomenclature

Symbols

J_F	UF filtrate flux (L/m^2 h)
μ	feed water viscosity (Pa·s)
ΔP	transmembrane pressure drop across membrane (kPa)
Δt	filtration duration in a filtration/backwash cycle (h)
R_m	clean UF membrane hydraulic resistance (m^{-1})
R_{cake}	cake resistance (m^{-1})
R_{irr}	irreversible resistance (m^{-1})
ΔR_T	UF fouling resistance increase (m^{-1})
R_{final}	final UF filtration resistance (m^{-1})
$R_{initial}$	initial UF filtration resistance (m^{-1})
ΔR_{BW}	unbackwashed resistance (m^{-1})
ΔR_{UB}	unbackwashed resistance (m^{-1})
FR	filtration period fouling rate (m^{-1} h^{-1})
BW_{eff}	backwash efficiency for cycle n (%)
R_{PB}	post-backwash resistance (m^{-1})
dR_{PB}/dt	post-backwash fouling rate (m^{-1} h^{-1})
C_{FeCl3}	concentration of $FeCl_3$ (mg/L)
Y_{UF}	UF recovery (%)
Δt_{BW}	backwash time (h)
J_{BW}	backwash flux ($L/m^2{\cdot}h$)
l_c	effective cake thickness (m)
$< >_j$	Averaged value for j^{th} segment

Subscript

n	indicate for the n^{th} cycle in filtration period
N	denote at the end of N cycles
j	filtration/backwash cycles moving average segment
i	initial value
o	base line value

Acknowledgements

This work was funded, in part, by the United States Office of Naval Research (N00014-11-1-0950 ONR and ONR N00014-09-1-1132), California Department of Water Resources (46-4120 and RD-2006-09), U.S. Bureau of Reclamation (R13AC80025), Naval Facilities Engineering Command (N62583-11-C-0630), and UCLA Water Technology Research (WaTeR) Center. Also acknowledged are the equipment and materials contributions for the UF-RO plant construction by Danfoss Sea Recovery (Henrik Wendelboe and Christopher Okada), Inge GmbH (Peter Berg, Martin Heijnen, and Josef Wunram), George Fisher (Rick Hines), Dow Water & Process Solutions (Michael Kim), and Ahlstrom (Rod Komlenic and Denise Russell). The authors also acknowledge the technical assistance during the field study by personnel of the Naval Facilities Engineering and Expeditionary Warfare Center (NAVFAC EXWC) at Port Hueneme, CA, William Varnava, Mark Miller, Paul Giuffrida, Theresa Hoffard, Joseph Saenz, and Micah Ing.

Appendix A. Supplementary data

Supplementary data to this article can be found online at https://doi.org/10.1016/j.desal.2017.11.038.

References

[1] H. Carrão, G. Naumann, P. Barbosa, Mapping global patterns of drought risk: an empirical framework based on sub-national estimates of hazard, exposure and vulnerability, Glob. Environ. Chang. 39 (2016) 108–124.
[2] A.K. Misra, Climate change and challenges of water and food security, Int. J. Sustain. Built Environ. 3 (2014) 153–165.
[3] M. Elimelech, W.A. Phillip, The future of seawater desalination: energy, technology, and the environment, Science 333 (2011) 712–717.
[4] H.C. Flemming, G. Schaule, T. Griebe, J. Schmitt, A. Tamachkiarowa, Biofouling—the Achilles heel of membrane processes, Desalination 113 (1997) 215–225.
[5] S. Gray, R. Semiat, M. Duke, A. Rahardianto, Y. Cohen, 4.04 - seawater use and desalination technology A2 - Wilderer, Peter, Treatise on Water Science, Elsevier, Oxford, 2011, pp. 73–109.
[6] L. Henthorne, B. Boysen, State-of-the-art of reverse osmosis desalination pretreatment, Desalination 356 (2015) 129–139.
[7] L.O. Villacorte, S.A.A. Tabatabai, D.M. Anderson, G.L. Amy, J.C. Schippers, M.D. Kennedy, Seawater reverse osmosis desalination and (harmful) algal blooms, Desalination 360 (2015) 61–80.
[8] B. Ghernaout, D. Ghernaout, A. Saiba, Algae and cyanotoxins removal by coagulation/flocculation: a review, Desalin. Water Treat. 20 (2010) 133–143.
[9] D.F. Halpern, J. McArdle, B. Antrim, Desalination and the environment UF pretreatment for SWRO: pilot studies, Desalination 182 (2005) 323–332.
[10] R. Schurer, A. Tabatabai, L. Villacorte, J.C. Schippers, M.D. Kennedy, Three years operational experience with ultrafiltration as SWRO pre-treatment during algal bloom, Desalin. Water Treat. 51 (2013) 1034–1042.
[11] K. Chua, M. Hawlader, A. Malek, Pretreatment of seawater: results of pilot trials in Singapore, Desalination 159 (2003) 225–243.
[12] R. Schurer, A. Janssen, L. Villacorte, M. Kennedy, Performance of ultrafiltration and coagulation in an UF-RO seawater desalination demonstration plant, Desalin. Water Treat. 42 (2012) 57–64.
[13] C.Y. Tang, T.H. Chong, A.G. Fane, Colloidal interactions and fouling of NF and RO membranes: a review, Adv. Colloid Interf. Sci. 164 (2011) 126–143.
[14] M. Wilf, M.K. Schierach, Improved performance and cost reduction of RO seawater systems using UF pretreatment, Desalination 135 (2001) 61–68.
[15] A. Brehant, V. Bonnelye, M. Perez, Comparison of MF/UF pretreatment with conventional filtration prior to RO membranes for surface seawater desalination, Desalination 144 (2002) 353–360.
[16] K. Burashid, A.R. Hussain, R.O. Seawater, plant operation and maintenance experience: Addur desalination plant operation assessment, Desalination 165 (2004) 11–22.
[17] O. Lorain, B. Hersant, F. Persin, A. Grasmick, N. Brunard, J.M. Espenan, Ultrafiltration membrane pre-treatment benefits for reverse osmosis process in seawater desalting. Quantification in terms of capital investment cost and operating cost reduction, Desalination 203 (2007) 277–285.
[18] P.H. Wolf, S. Siverns, S. Monti, UF membranes for RO desalination pretreatment, Desalination 182 (2005) 293–300.
[19] L.X. Gao, H. Gu, A. Rahardianto, P.D. Christofides, Y. Cohen, Self-adaptive cycle-to-cycle control of in-line coagulant dosing in ultrafiltration for pre-treatment of reverse osmosis feed water, Desalination 401 (2017) 22–31.
[20] S. Delgado Díaz, L. Vera Peña, E. González Cabrera, M. Martínez Soto, L.M. Vera Cabezas, L.R. Bravo Sánchez, Effect of previous coagulation in direct ultrafiltration of primary settled municipal wastewater, Desalination 304 (2012) 41–48.
[21] E. Friedler, I. Katz, C.G. Dosoretz, Chlorination and coagulation as pretreatments for greywater desalination, Desalination 222 (2008) 38–49.
[22] K. Kimura, K. Tanaka, Y. Watanabe, Microfiltration of different surface waters with/without coagulation: clear correlations between membrane fouling and hydrophilic biopolymers, Water Res. 49 (2014) 434–443.
[23] S.A.A. Tabatabai, J.C. Schippers, M.D. Kennedy, Effect of coagulation on fouling potential and removal of algal organic matter in ultrafiltration pretreatment to seawater reverse osmosis, Water Res. 59 (2014) 283–294.
[24] J. Wang, J. Guan, S.R. Santiwong, T.D. Waite, Characterization of floc size and structure under different monomer and polymer coagulants on microfiltration membrane fouling, J. Membr. Sci. 321 (2008) 132–138.
[25] D. Gille, W. Czolkoss, Desalination and the environment ultrafiltration with multibore membranes as seawater pre-treatment, Desalination 182 (2005) 301–307.
[26] A. Jezowska, A. Bottino, G. Capannelli, C. Fabbri, G. Migliorini, Ultrafiltration as direct pre-treatment of seawater - a case study, Desalination 245 (2009) 723–729.
[27] N. Porcelli, S. Judd, Chemical cleaning of potable water membranes: a review, Sep. Purif. Technol. 71 (2010) 137–143.
[28] Y.C. Woo, J.J. Lee, L.D. Tijing, H.K. Shon, M. Yao, H.-S. Kim, Characteristics of membrane fouling by consecutive chemical cleaning in pressurized ultrafiltration as pre-treatment of seawater desalination, Desalination 369 (2015) 51–61.
[29] C. Regula, E. Carretier, Y. Wyart, G. Gésan-Guiziou, A. Vincent, D. Boudot, P. Moulin, Chemical cleaning/disinfection and ageing of organic UF membranes: a review, Water Res. 56 (2014) 325–365.
[30] X. Shi, G. Tal, N.P. Hankins, V. Gitis, Fouling and cleaning of ultrafiltration membranes: a review, J. Water Process Eng. 1 (2014) 121–138.
[31] N.G. Cogan, J. Li, A.R. Badireddy, S. Chellam, Optimal backwashing in dead-end bacterial microfiltration with irreversible attachment mediated by extracellular polymeric substances production, J. Membr. Sci. 520 (2016) 337–344.
[32] H. Gu, A. Rahardianto, L.X. Gao, P.D. Christofides, Y. Cohen, Ultrafiltration with self-generated RO concentrate pulse backwash in a novel integrated seawater desalination UF-RO system, J. Membr. Sci. 520 (2016) 111–119.
[33] A. Lok, H. Wray, P. Bérubé, R.C. Andrews, Optimization of air sparging and in-line coagulation for ultrafiltration fouling control, Sep. Purif. Technol. 188 (2017) 60–66.
[34] L.X. Gao, A. Rahardianto, H. Gu, P.D. Christofides, Y. Cohen, Novel design and operational control of integrated ultrafiltration - reverse osmosis system with RO concentrate backwash, Desalination 382 (2016) 43–52.
[35] E. Akhondi, F. Zamani, A.W.K. Law, W.B. Krantz, A.G. Fane, J.W. Chew, Influence of backwashing on the pore size of hollow fiber ultrafiltration membranes, J. Membr. Sci. 521 (2017) 33–42.

[36] H. Chang, H. Liang, F. Qu, S. Shao, H. Yu, B. Liu, W. Gao, G. Li, Role of backwash water composition in alleviating ultrafiltration membrane fouling by sodium alginate and the effectiveness of salt backwashing, J. Membr. Sci. 499 (2016) 429–441.
[37] H. Chang, B. Liu, P. Yang, Q. Wang, K. Li, G. Li, H. Liang, Salt backwashing of organic-fouled ultrafiltration membranes: effects of feed water properties and hydrodynamic conditions, J. Water Process Eng. (2017), http://dx.doi.org/10.1016/j.jwpe.2017.06.012 in press.
[38] Y. He, J. Sharma, R. Bogati, B. Liao, C. Goodwin, K. Marshall, Impacts of aging and chemical cleaning on the properties and performance of ultrafiltration membranes in potable water treatment, Sep. Sci. Technol. 49 (2014) 1317–1325.
[39] S.A.A. Tabatabai, M.D. Kennedy, G.L. Amy, J.C. Schippers, Optimizing inline coagulation to reduce chemical consumption in MF/UF systems, Desalin. Water Treat. 6 (2009) 94–101.
[40] A. Alhadidi, A.J.B. Kemperman, B. Blankert, J.C. Schippers, M. Wessling, W.G.J. van der Meer, Silt Density Index and Modified Fouling Index relation, and effect of pressure, temperature and membrane resistance, Desalination 273 (2011) 48–56.
[41] A. Alhadidi, A.J.B. Kemperman, R. Schurer, J.C. Schippers, M. Wessling, W.G.J. van der Meer, Using SDI, SDI + and MFI to evaluate fouling in a UF/RO desalination pilot plant, Desalination 285 (2012) 153–162.
[42] S.F.E. Boerlage, M. Kennedy, Z. Tarawneh, R. De Faber, J.C. Schippers, Development of the MFI-UF in constant flux filtration, Desalination 161 (2004) 103–113.
[43] S.F.E. Boerlage, M.D. Kennedy, M.R. Dickson, D.E.Y. El-Hodali, J.C. Schippers, The modified fouling index using ultrafiltration membranes (MFI-UF): characterisation, filtration mechanisms and proposed reference membrane, J. Membr. Sci. 197 (2002) 1–21.
[44] K. Hong, S. Lee, S. Choi, Y. Yu, S. Hong, H. Moon, J. Sohn, J. Yang, Assessment of various membrane fouling indexes under seawater conditions, Desalination 247 (2009) 247–259.
[45] H. Huang, T.A. Young, J.G. Jacangelo, Unified membrane fouling index for low pressure membrane filtration of natural waters: principles and methodology, Environ. Sci. Technol. 42 (2008) 714–720.
[46] R.M. Rachman, N. Ghaffour, F. Wali, G.L. Amy, Assessment of silt density index (SDI) as fouling propensity parameter in reverse osmosis (RO) desalination systems, Desalin. Water Treat. 51 (2013) 1091–1103.
[47] S.G. Salinas-Rodriguez, G.L. Amy, J.C. Schippers, M.D. Kennedy, The Modified Fouling Index Ultrafiltration constant flux for assessing particulate/colloidal fouling of RO systems, Desalination 365 (2015) 79–91.
[48] M. Zupancic, D. Novak, J. Diaci, I. Golobic, An evaluation of industrial ultrafiltration systems for surface water using fouling indices as a performance indicator, Desalination 344 (2014) 321–328.
[49] A. Massé, O. Arab, V. Séchet, P. Jaouen, M. Pontié, N.-E. Sabiri, S. Plantier, Performances of dead-end ultrafiltration of seawater: from the filtration and backwash efficiencies to the membrane fouling mechanisms, Sep. Purif. Technol. 156 (Part 2) (2015) 512–521.
[50] S. Jeong, S. Vigneswaran, Practical use of standard pore blocking index as an indicator of biofouling potential in seawater desalination, Desalination 365 (2015) 8–14.
[51] K. Chinu, S. Vigneswaran, L. Erdei, H.K. Shon, J. Kandasamy, H.H. Ngo, Comparison of fouling indices in assessing pre-treatment for seawater reverse osmosis, Desalin. Water Treat. 18 (2010) 187–191.
[52] S.A. Alizadeh Tabatabai, J.C. Schippers, M.D. Kennedy, Effect of coagulation on fouling potential and removal of algal organic matter in ultrafiltration pretreatment to seawater reverse osmosis, Water Res. 59 (2014) 283–294.
[53] C.-H. Wei, S. Laborie, R. Ben Aim, G. Amy, Full utilization of silt density index (SDI) measurements for seawater pre-treatment, J. Membr. Sci. 405 (2012) 212–218.
[54] H.K. Shon, S.H. Kim, S. Vigneswaran, R. Ben Aim, S. Lee, J. Cho, Physicochemical pretreatment of seawater: fouling reduction and membrane characterization, Desalination 238 (2009) 10–21.
[55] A. Resosudarmo, Y. Ye, P. Le-Clech, V. Chen, Analysis of UF membrane fouling mechanisms caused by organic interactions in seawater, Water Res. 47 (2013) 911–921.
[56] T. Berman, R. Mizrahi, C.G. Dosoretz, Transparent exopolymer particles (TEP): a critical factor in aquatic biofilm initiation and fouling on filtration membranes, Desalination 276 (2011) 184–190.
[57] S.Q. Huang, N. Voutchkov, S.C. Jiang, Investigation of environmental influences on membrane biofouling in a Southern California desalination pilot plant, Desalination 319 (2013) 1–9.
[58] Y. Liu, X. Li, Y. Yang, S. Liang, Fouling control of PAC/UF process for treating algal-rich water, Desalination 355 (2015) 75–82.
[59] Y. Zhang, J. Tian, J. Nan, S. Gao, H. Liang, M. Wang, G. Li, Effect of PAC addition on immersed ultrafiltration for the treatment of algal-rich water, J. Hazard. Mater. 186 (2011) 1415–1424.
[60] K. Glucina, A. Alvarez, J.M. Laîné, Membranes in Drinking and Industrial Water Production Assessment of an integrated membrane system for surface water treatment, Desalination 132 (2000) 73–82.
[61] S. Jeong, F. Nateghi, T.V. Nguyen, S. Vigneswaran, T.A. Tu, Pretreatment for seawater desalination by flocculation: performance of modified poly ferric silicate (PFSi-delta) and ferric chloride as flocculants, Desalination 283 (2011) 106–110.
[62] P. Lipp, M. Witte, G. Baldauf, A.A. Povorov, Membranes in Drinking and Industrial Water Production Treatment of reservoir water with a backwashable MF/UF spiral wound membrane, Desalination 179 (2005) 83–94.
[63] A.H. Nguyen, J.E. Tobiason, K.J. Howe, Fouling indices for low pressure hollow fiber membrane performance assessment, Water Res. 45 (2011) 2627–2637.
[64] L. Gao, A. Rahardianto, H. Gu, P.D. Christofides, Y. Cohen, Energy-optimal control of RO desalination, Ind. Eng. Chem. Res. 53 (2014) 7409–7420.
[65] E. Zondervan, B. Blankert, B.H.L. Betlem, B. Roffel, Development of a multi-objective coagulation system for long-term fouling control in dead-end ultrafiltration, J. Membr. Sci. 325 (2008) 823–830.
[66] Y. Cohen, P.D. Christofides, A. Rahardianto, A.R. Bartman, A. Zhu, H. Gu, L.X. Gao, Apparatus, system and method for integrated filtration and reverse osmosis desalination, US Patent, US20140048462 A1, US 13/822,622 (2014).
[67] D.M. Anderson, J.M. Burkholder, W.P. Cochlan, P.M. Glibert, C.J. Gobler, C.A. Heil, R.M. Kudela, M.L. Parsons, J.J. Rensel, D.W. Townsend, Harmful algal blooms and eutrophication: examining linkages from selected coastal regions of the United States, Harmful Algae 8 (2008) 39–53.
[68] R.A. Horner, D.L. Garrison, F.G. Plumley, Harmful algal blooms and red tide problems on the US west coast, Limnol. Oceanogr. 42 (1997) 1076–1088.
[69] G. Belfort, R.H. Davis, A.L. Zydney, The behavior of suspensions and macromolecular solutions in crossflow microfiltration, J. Membr. Sci. 96 (1994) 1–58.
[70] J.-D. Lee, S.-H. Lee, M.-H. Jo, P.-K. Park, C.-H. Lee, J.-W. Kwak, Effect of coagulation conditions on membrane filtration characteristics in coagulation – microfiltration process for water treatment, Environ. Sci. Technol. 34 (2000) 3780–3788.
[71] M. Yao, J. Nan, T. Chen, D. Zhan, Q. Li, Z. Wang, H. Li, Influence of flocs breakage process on membrane fouling in coagulation/ultrafiltration process—effect of additional coagulant of poly-aluminum chloride and polyacrylamide, J. Membr. Sci. 491 (2015) 63–72.